Title

Interaction of diazonamide A with tubulin

Authors

Bai, Ruoli
Cruz-Monserrate, Zobeida
Fenical, William
et al.

Publication Date

2020-02-01

DOI

10.1016/j.abb.2019.108217

Peer reviewed

HHS Public Access

Author manuscript

Arch Biochem Biophys. Author manuscript; available in PMC 2021 February 15.

Published in final edited form as:

Arch Biochem Biophys. 2020 February 15; 680: 108217. doi:10.1016/j.abb.2019.108217.

INTERACTION OF DIAZONAMIDE A WITH TUBULIN

Ruoli Bai[a], **Zobeida Cruz-Monserrate**[a], **William Fenical**[b], **George R. Pettit**[c], **Ernest Hamel**[a]

[a]Screening Technologies Branch, Developmental Therapeutics Program, Division of Cancer Treatment and Diagnosis, Frederick National Laboratory for Cancer Research, National Cancer Institute, National Institutes of Health, Frederick, MD, 21702, USA

[b]Center for Marine Biotechnology and Biomedicine, Scripps Institution of Oceanography, University of California at San Diego, La Jolla, CA, 92093, USA

[c]Laboratory for Discovery of Anti-Cancer and Anti-Infective Drugs, School of Molecular Sciences, Arizona State University, Tempe, AZ, 85287, USA

Abstract

[^{3}H]Diazonamide A ([^{3}H]DZA), prepared from the natural product isolated from *Diazona angulata*, bound to tubulin in larger aberrant assembly products (> 500 kDa by sizing HPLC) but not to the α,β-tubulin heterodimer. The binding reaction was rapid, but stoichiometry was low. Stoichiometry was enhanced up to 8-fold by preincubating the tubulin in the reaction mixture prior to adding the [^{3}H]DZA. Although Mg^{2+} did not affect binding stoichiometry, the cation markedly increased the number of tubulin rings (diameter about 50 nm) observed by negative stain electron microscopy. Bound [^{3}H]DZA did not dissociate from the tubulin oligomers despite extensive column chromatography but did dissociate in the presence of 8 M urea. With preincubated tubulin, a superstoichiometric amount of [^{3}H]DZA appeared to bind to the tubulin oligomeric structures, consistent with observations that neither nonradiolabeled DZA nor DZA analogues inhibited binding of [^{3}H]DZA to the tubulin oligomers. Only weak inhibition of binding was observed with multiple antimitotic compounds. In particular, no inhibition occurred with vinblastine, and the best inhibitors of those examined were dolastatin 10 and cryptophycin 1. We compared the aberrant assembly reaction induced by DZA to those induced by other antimitotic peptides and depsipeptides, in particular dolastatin 10, cryptophycin 1, and hemiasterlin, but the results obtained varied considerably in terms of requirements for maximal reactions, polymer morphology, and inhibitory effects observed with antimitotic compounds.

Corresponding author: Dr. E. Hamel, Building 322, Room 102, P. O. Box B, Frederick National Laboratory for Cancer Research, Frederick MD 21702. hamele@mail.nih.gov.

Author statement:

Ruoli Bai planned and performed experiments and analyzed data.

Zobeida Cruz-Monserrate planned and performed experiments, analyzed data, and reviewed and edited the manuscript.

William Fenical led the team that isolated and characterized diazonamide A and reviewed and edited the manuscript.

George R. Pettit led the team that isolated and characterized dolastatin 10 and other compounds used in the project and reviewed and edited the manuscript.

Ernest Hamel led the project, planned and performed experiments, analyzed data, and wrote much of the text of the manuscript.

1. Introduction

Natural product antimitotic peptides and depsipeptides include a number of potently cytotoxic agents, most notably cryptophycin 1 [1,2] and the tubulysins [3], both of which yield picomolar IC_{50} values for cultured cancer cells. The antimitotic (depsi)peptides display a great deal of structural variation (see structures in ref. 4), but one common feature is that they all contain unusual amino acid residues. In this report, we will describe our findings with radiolabeled diazonamide A (DZA; structure in Fig. 1), originally isolated from the ascidian *Diazona angulata* [5,6]. In the course of these studies, we found that the radiolabel could not be detected bound to the αβ-tubulin heterodimer, but only to larger aggregates of the protein. While aberrant assembly products induced by antimitotic (depsi)peptides have long been described [7-11], as far as we know the polymers induced by DZA have not been reported previously. We devoted some attention to these polymers, comparing the DZA-induced reaction to those induced by other (depsi)peptides, with some of our findings presented in the Supplemental Materials to this paper.

DZA was first found to have apparent antitubulin activity at the cellular level, showing (1) a tubulin active agent pattern in differential cytotoxicity data analyzed by the COMPARE algorithm [12], (2) disruption of intracellular microtubules, and (3) accumulation of cells arrested in the G2/M phase of the cell cycle [13]. We then showed that DZA was a potent inhibitor of tubulin assembly [14], but it had negligible effects on the binding of other ligands to tubulin (radiolabeled colchicine, vinblastine, dolastatin 10 [D10], and GTP) [6]. Synthetic DZA and structural analogues were subsequently shown by Wang et al. [15] to interact with ornithine δ-amino transferase, and these authors proposed that this enzyme played an unsuspected role in mitosis and was the intracellular target of DZA rather than tubulin. Later, Wieczorek et al. [16] described a crystal structure of a DZA analogue (DZ-2384; structure in Fig. 1) bound to tubulin complexed with a stathmin fragment and tubulin tyrosine ligase. In this structure, formed with high concentrations of tubulin and the analogue, the DZA analogue bound in the vinblastine site. Subsequently, Sáez-Calvo et al. [17] described a group of polycyclic compounds called triazolopyrimidines (TPs) with unusual properties. A previously studied analogue had strongly inhibited vinblastine binding to tubulin [18]. In a crystal structure of the most active TP compound bound to tubulin in the vinblastine site, Sáez-Calvo et al. [17] noted that there was extensive overlap between this TP and DZ-2384 in their crystal structures. In cells, however, instead of causing the disappearance of microtubules, the TPs caused increased microtubule formation and formation of microtubule bundles as is observed with taxoid site and laulimalide site agents. In vitro, however, while the TPs bound to preformed microtubules and stabilized them, when added to tubulin they caused an aberrant assembly reaction with formation of helical polymers when higher TP concentrations were used. With lower TP concentrations, microtubules were formed. The maximum TP stoichiometry observed in the helical polymers was 0.8, but the stoichiometry of TP bound to microtubules was much lower because of the reduced drug input (5% of the tubulin concentration).

To obtain additional evidence as to whether or not DZA, as indicated by its classical antitubulin cellular effects, its potent inhibition of tubulin assembly (one of the most potent assembly inhibitors we have studied), and the recent crystal structure with DZ-2384, could

interact with tubulin, we had the natural product DZA tritiated. The [^{3}H]DZA did bind to tubulin, but the binding reaction differed significantly from those we have previously examined. The stoichiometry of binding was very low, until we discovered that the binding reaction was substantially enhanced by preincubating tubulin in the reaction mixture prior to addition of the [^{3}H]DZA. By size exclusion high performance liquid chromatography (HPLC) analysis, we found that radiolabel was only recovered in the void volume, with no apparent binding to either the αβ-tubulin dimer or to smaller aggregates represented by included peaks in the column eluate. This agreed with electron microscopy findings, which showed that DZA induced the formation, from purified tubulin, of rings that were approximately 50 nm in diameter, in contrast to the smaller rings previously observed with D10, cryptophycin 1, and hemiasterlin [11].

2. Materials and methods

2.1. Materials

Electrophoretically homogeneous bovine brain tubulin was purified as described before [19]. This tubulin was used in the turbidimetric and pelleting studies presented here. Tubulin used in the ligand binding studies and in electron microscopy underwent gel filtration chromatography on Sephadex G-50 (superfine) to remove unbound nucleotide [20]. DZA was obtained from *Diazona angulata* as described previously [5,13]. The natural product was tritiated at AmBios Labs, and the [^{3}H]DZA had a specific activity of 2.0 Ci/mmol. Synthetic D10 [21] and combretastatin A-4 [22] were prepared as described previously. Natural hemiasterlin [23] and spongistatin 1 [24] were obtained as described previously. Natural cryptophycin 1 was generously provided by Merck Research Laboratories. The Drug Synthesis & Chemistry and Natural Products Branches, Developmental Therapeutics Program, National Cancer Institute generously provided auristatin PE (a D10 analogue) and natural halichondrin B, maytansine, vinblastine, and [^{3}H]D10. Podophyllotoxin was obtained from Aldrich. DZA analogues 1 and 2 were generously provided by Dr. P. G. Harran, University of California at Los Angeles (see below for structures). Stock solutions of all antimitotic compounds were prepared in dimethyl sulfoxide, and an equivalent concentration of dimethyl sulfoxide was included in control reaction mixtures.

2.2. Biochemical and electron microscopic methods

All reaction mixtures contained 0.1 M 4-morpholineethanesulfonate (Mes), taken from a 1.0 M stock solution adjusted to pH 6.9 or pH 6.5 with NaOH. Other components will be described in the individual experiments. We used gel filtration (Sephadex G-50 superfine) in syringe-columns [25] and size exclusion HPLC to examine the binding of [^{3}H]DZA to purified tubulin. With the syringe-columns, protein and bound [^{3}H]DZA in column filtrates were determined by the Lowry assay and liquid scintillation counting in glass vials of aliquots of each filtrate to obtain binding stoichiometry values. The syringe-columns were prepared in polypropylene tuberculin syringe barrels with polyethylene discs closing their outlets. HPLC was performed at room temperature on a Shodex KW-803 column (6 x 300 mm, up to three in series in some experiments) with a Shodex KWG guard column (6 x 50 mm), using an Agilent Technologies system in-line with a LabLogic β-RAM model 3 flow detector. The outflow of the column was analyzed for protein by A_{280} and for radiolabel. For

negative stain electron microscopy, a droplet (5-10 μL) was placed on a carbon-coated Formvar-treated, 200-mesh copper grid, followed by a rapid succession of drops of 0.5% (w/v) uranyl acetate. Excess stain was wicked from the grid with torn filter paper, and the grids were air-dried. They were subsequently examined in a Zeiss model 10CA electron microscope. Glass reaction vessels were used in all experiments, but polypropylene pipette tips were used to transfer all reaction components into the reaction vessels and to transfer samples from the reaction vessels to the syringe-columns.

3. Results

3.1. Initial studies with [^{3}H]DZA

Using gel filtration in syringe-columns [25] to examine the binding of [^{3}H]DZA to purified tubulin, we observed low stoichiometry of binding (Table 1, Reaction Condition 1). Among the reaction parameters we examined, trying to improve binding stoichiometry, were time, pH (in the pH 6-7 range), buffer component, and addition of Mg^{2+} (see Table 2), GTP or GDP to the reaction mixture. None of the parameters changed the stoichiometry of binding. Despite the low binding stoichiometry, we examined the effects of several inhibitors of tubulin assembly on the binding of [^{3}H]DZA to tubulin, and no significant inhibition occurred. In an effort to increase inhibitory effects, we preincubated the potential inhibitors with tubulin prior to addition of [^{3}H]DZA (see below), including a preincubated tubulin control. We observed a marked increase in the stoichiometry of binding of [^{3}H]DZA in the control reaction mixture.

Table 1 summarizes three reaction conditions exploring this phenomenon. While the preincubation of the final tubulin solution for 1 h at room temperature (22 °C) prior to addition of the [^{3}H]DZA led to an almost 8-fold increase in binding stoichiometry, most of this increase (almost 6-fold) occurred after simply diluting the stock tubulin solution (65 mg/mL) to the final concentration of 0.4 mg/mL (4.0 μM) and immediately adding the [^{3}H]DZA. This implies there might be a conformational change that occurs with the tubulin upon dilution.

Table 2 demonstrates that both 0.5 and 2.0 mM $MgCl_2$ had little effect on the amount of [^{3}H]DZA bound to tubulin either with or without a preincubation, and the preincubation effects were similar under the three reaction conditions examined. While we have frequently used 0.5 mM Mg^{2+} in our tubulin studies, the 2.0 mM concentration was also used in this experiment because of the dramatic effects, described below, it had on the abundance and morphology of DZA-induced tubulin rings.

As for the change in tubulin, a possibility that we considered was disassembly of preexisting tubulin rings, which have been described by numerous investigators [26-31]. We have observed such rings repeatedly in our tubulin preparations, including the preparation used in these studies. In Fig. 2 are examples of rings found in a tubulin solution diluted to 0.4 mg/mL in 0.1 M Mes (pH 6.9), with the negatively stained sample prepared as soon as possible after the reaction mixture was prepared. These rings tended to be widely scattered, but occasionally several rings could be found in a single electron microscopic field, as is the case with those shown in Fig. 2. We observed only what appeared to be single rings, average

diameter 40.6 nm, with no double rings visualized in 0.1 M Mes (pH 6.9). After 2 h at room temperature, we could not find any rings (2 independent experiments), consistent with the idea that ring disassembly was an important event during the preincubation leading to increased binding of [^{3}H]DZA.

In addition, we examined the effect of 0.5 mM Mg^{2+} on preexisting rings. The rings did not appear to be more abundant at this Mg^{2+} concentration, but they did seem to be more stable, not disappearing as extensively as without Mg^{2+}, and there were also double rings observed in the presence of 0.5 mM Mg^{2+}.

3.2. Kinetics of [^{3}H]DZA binding to tubulin

We attempted to perform a time course study of the binding of [^{3}H]DZA to tubulin, following tubulin preincubation, and the reaction was very rapid. The samples processed as rapidly as possible (we estimate representing a 20-30 s time point) bound about 75% as much of the ligand as was bound at later time points (Table 3).

Binding to tubulin as a function of DZA concentration was examined without a preincubation and with a 90 min preincubation. The data obtained are presented in Fig. 3. Under both reaction conditions, there was a steady increase in the stoichiometry of binding as the DZA concentration increased, with no evidence that the compound concentration was approaching saturation. As in the studies presented above, there was a marked increase when the diluted tubulin was preincubated. Moreover, at the highest DZA concentration examined (20 μM), the amount of compound bound to tubulin was superstoichiometric (1.32 mol of [^{3}H]DZA bound per mol of tubulin). This implies more than one binding site for DZA on tubulin, in contrast to the substoichiometric binding observed with the TP derivatives [17]. The limited amounts of DZA that we possessed made further exploration of this observation impossible, but consistent with this finding is that, in our initial experiments with [^{3}H]DZA, we observed no inhibition of binding by nonradiolabeled DZA. In addition, in HPLC experiments presented below, we observed an apparent stoichiometry of 1.96 when 8 μM [^{3}H]DZA was incubated with 2 μM tubulin.

The data of Fig. 3, together with experiments under other reaction conditions, were plotted in the Scatchard format, together with a repetition of the previously published experiment with [^{3}H]D10 [8] (Fig. 4). As before [8], D10 yielded a biphasic Scatchard plot, which was interpreted in terms of formation of small oligomers leading to formation of ever larger aggregates, in parallel with the action of vinblastine [8,32]. DZA binding, however, at all concentrations examined, yielded a Scatchard plot with minimal slope. In view of the HPLC binding data (see below), such a Scatchard plot might indicate that an antitubulin compound will only bind to larger assemblies of tubulin, as opposed to αβ-dimers or small oligomers.

3.3. Aberrant assembly reactions induced by antimitotic (depsi)peptides

Of the peptidic compounds we had studied previously (D10, cryptophycin 1, hemiasterlin) [8-10], the most dramatic aberrant assembly occurred with D10. This peptide caused formation of milky solutions of tubulin, and hemiasterlin or cryptophycin 1 could either inhibit or enhance turbidity development, depending on reaction conditions. In fact, the D10-induced aberrant assembly product could be readily harvested by centrifugation

(Supplemental Materials, Fig. 1; 0.1 M Mes [pH 6.9] + 0.5 mM $MgCl_2$), and only vinblastine, of the compounds examined, also produced an aberrant assembly product that could be recovered by centrifugation, although a higher concentration of vinblastine than of D10 was required (Supplemental Materials, Table 1).

We also examined inhibitory effects of multiple compounds on D10-induced aberrant polymer formation (Supplemental Materials, Fig. 2). Potent inhibition (IC_{50} < 10 μM) occurred with spongistatin 1, maytansine, cryptophycin 1, and DZA. A complete table of the IC_{50} values obtained will be presented and discussed below.

We studied the effects of a variety of reaction parameters on turbidity development induced by antimitotic (depsi)peptides, and the greatest effects were observed with changes in temperature, pH, and Mg^{2+} concentration. Extensive turbidity development occurred with D10 under all conditions examined, but Supplemental Materials, Fig. 3, shows the effects of varying all three parameters on turbidity development with cryptophycin 1 (Panel A), hemiasterlin (panel B), and DZA (Panel C). Cryptophycin 1 showed little turbidity development under most conditions examined, but when the reaction pH was lowered to pH 6.5 and the Mg^{2+} concentration raised to 10 mM, we observed turbidity development at 0 °C that decreased as the reaction temperature rose. A similar pattern was observed with hemiasterlin, but only 2 mM Mg^{2+} was required. With DZA, turbidity development did not require a change in pH, but did require increased Mg^{2+} (2 mM). In contrast to the other two compounds, however, turbidity development with DZA increased with temperature.

Furthermore, with DZA, simply changing the reaction pH to 6.5 resulted in much more extensive turbidity development, even at 22 °C (Supplemental Materials, Fig. 4). In fact, turbidity development with DZA differed little from that with D10 under the reaction condition (0.1 M Mes [pH 6.5], 2 mM $MgCl_2$, 22 °C) used for the experiments presented in Supplemental Materials, Fig. 4. However, as in earlier studies with cryptophycin 1 [9] and hemiasterlin [10], where turbidimetric and electron microscopic evidence of aberrant polymers were not concordant, we found that DZA-induced polymer that could be harvested by centrifugation was not necessarily concordant with turbidimetry. Not only could almost all the tubulin in the reaction mixture be recovered in pellets at pH 6.5/2 mM $MgCl_2$/22 °C, but substantial tubulin could also be recovered at pH 6.9/2 mM $MgCl_2$/22 °C, where there was little change in turbidity (Supplemental Materials, Fig. 3C). We therefore used this reaction condition in centrifugation experiments with DZA analogous to those with D10 (presented in Supplemental Materials, Fig. 2, and Supplemental Materials, Table 1) to minimize reaction condition differences.

Supplemental Materials, Table 2, presents the effects of different compounds on tubulin recovery by centrifugation, with large amounts recovered with 10 and 20 μM DZA, even larger amounts with 10 and 20 μM D10 and 20 μM vinblastine, and a moderate amount with 20 μM hemiasterlin. Note the discordance between the turbidity observed with hemiasterlin (Supplemental Materials, Fig. 3B) and DZA (Supplemental Materials, Fig. 3C) and the size of the pellets obtained under the same reaction condition. In Supplemental Materials, Fig. 5, we show that almost every compound examined inhibited pellet formation induced by 10 μM DZA. Again, IC_{50} values will be presented and discussed below.

3.4. Electron microscopic observations of DZA-induced aberrant polymer

We examined by negative stain electron microscopy aberrant tubulin polymers formed in the presence of DZA under four reaction conditions: in 0.1 M Mes, pH 6.9 or 6.5, with or without 2 mM $MgCl_2$. No major difference was observed between the two pH's, with scattered rings observed at both pH 6.9 and 6.5 (Fig. 5AB). At both pH's there was a marked increase in the abundance of rings observed with 2 mM $MgCl_2$ (Fig. 5CD). The Mg^{2+} effect was observed in four independent experiments. No similar effect of Mg^{2+} was observed with D10-induced rings in contemporaneous experiments (shown in Supplemental Materials, Fig. 6, sample prepared without $MgCl_2$, average ring diameter 44.5 nm).

The rings formed in the presence of 2.0 mM Mg^{2+} with DZA appeared to have significantly thicker walls than those formed in the absence of Mg^{2+}, perhaps indicating double rings, but evaluation of the specimens at higher magnification did not improve ring resolution. The average diameters of rings were 46.7 (pH 6.9, no $MgCl_2$), 50.5 (pH 6.5, no $MgCl_2$), 55.1 (pH 6.9, 2 mM $MgCl_2$), and 55.7 (pH 6.5, 2 mM $MgCl_2$) nm.

3.5. Inhibitory effects of antimitotic compounds on [^{3}H]DZA binding to tubulin and comparison with inhibitory effects on tubulin pellet formation by DZA and D10

In Table 4 are summarized the inhibitory effects of a number of antitubulin compounds on the binding of [^{3}H]DZA to tubulin as measured by centrifugal gel filtration and on pellet formation induced by DZA or D10. The purpose of this comparison was to determine whether any insight might be gained into the binding site of DZA on tubulin.

The most potent inhibitors of [^{3}H]DZA binding were D10 and cryptophycin 1, with hemiasterlin less active. Concentration studies were performed with D10 and cryptophycin 1, and 50% of maximal inhibition (as an IC_{50} equivalent) occurred with 0.9 μM D10 and 1.9 μM cryptophycin 1. Either compound at 3 μM resulted in near maximal inhibition, which was 50-60%, perhaps consistent with the superstoichiometric binding of [^{3}H]DZA described above (i.e., D10 and cryptophycin 1 can inhibit binding at one of two sites to which [^{3}H]DZA can bind). Vinblastine, on the other hand, had absolutely no inhibitory effect on the binding of [^{3}H]DZA, and in fact it had a small stimulatory effect. Weaker inhibition occurred with the macrocyclic polyethers halichondrin B and spongistatin 1. Minimal inhibition occurred with maytansine, and, somewhat surprisingly, the colchicine site inhibitors combretastatin A-4 and podophyllotoxin also had weak inhibitory effects. Two analogues of DZA (structures in Fig. 6) had the seemingly paradoxical effect of enhancing the binding of [^{3}H]DZA to tubulin, reminiscent of our inability to inhibit [^{3}H]DZA binding with nonradiolabeled DZA. These findings, too, are consistent with the superstoichiometric amount of [^{3}H]DZA bound to tubulin described above (i.e., nonradiolabeled DZA and the analogues can bind to an additional site or sites to which [^{3}H]DZA can bind).

There seemed to be little correlation of these effects on [^{3}H]DZA binding with inhibition of pellet formation induced by either DZA itself or D10. Perhaps most importantly, D10 strongly inhibited DZA-induced pellet formation, as did cryptophycin 1 and hemiasterlin. Vinblastine also was strongly inhibitory, as were maytansine and the two polyethers. The two colchicine site inhibitors were weakly inhibitory, with combretastatin A-4 more potent

than podophyllotoxin. D10-induced pellet formation displayed a wider range of effects. The strongest inhibition occurred with spongistatin 1 and maytansine, somewhat weaker effects with cryptophycin 1 and halichondrin B, while only weak inhibition was observed with vinblastine, DZA, and podophyllotoxin. Negligible inhibition was observed with hemiasterlin and combretastatin A-4.

In short, we did not gain any insight into a potential binding site for the [^{3}H]DZA from effects of the antitubulin compounds on pellet formation induced by DZA and D10. A possible complicating factor is the masking of binding sites when alternate aberrant polymer formation can occur with different agents.

3.6. Size exclusion HPLC indicates that binding of [^{3}H]DZA occurs only on larger tubulin assemblies

When we subjected mixtures of [^{3}H]DZA and tubulin to size exclusion HPLC, we obtained unexpected results. No matter what reaction condition we examined, radiolabel bound to protein only appeared in the void volume (Fig. 7). Moreover, the only protein peaks in the HPLC tracing were the void volume peak (> 500 kDa) and the 100 kDa αβ-tubulin dimer peak. In previously published studies with [^{3}H]halichondrin B [33], examined by this method, radiolabel only bound to the 100 kDa αβ-tubulin dimer peak. Earlier [8], using a different HPLC system and column, we had examined the binding of low concentrations of [^{3}H]D10 to tubulin, and we found radiolabel in a 200 kDa peak that we assumed was a complex of two αβ-dimers with one or two D10 molecules. With higher concentrations of [^{3}H]D10, all the tubulin and all protein-bound radiolabel was driven into the void volume peak. We were able to reproduce these findings with D10 with the current HPLC system (data not presented) and, further, identified what were probably 300, 400, and 500 kDa peaks in the included volume, as well as radiolabel in these larger species (Supplemental Materials, Fig. 7).

In contrast, with [^{3}H]DZA, we have been unable to demonstrate radiolabel in any oligomeric species, other than in the void volume peak. Another difference from D10 is that we were unable to drive all the αβ-dimer into the void volume peak with DZA, at least at compound to tubulin ratios up to 4. We had insufficient DZA to examine higher compound concentrations.

The areas of the radiolabeled peaks in the void volume and in the free drug peak retained by the HPLC column, together with the areas of 280 nm absorption in the void volume and the 100 kDa peak, permitted us to calculate an estimated stoichiometry for [^{3}H]DZA bound to tubulin. For the experiment shown in Fig. 7A, this estimate of stoichiometry is 0.13; for Fig. 7B, 0.57; and for Fig. 7C, 1.96. (These estimates ignore distortion of the void volume absorbance by potential light scattering of oligomeric structures and a potential contribution to absorbance by bound DZA.) Note again, that with the highest concentration of DZA used, a superstoichiometric amount of compound was bound to the tubulin oligomers.

We also found little change in the radiolabel in the void volume peak if the column volume was increased by adding a second and a third column in series. This was in contrast to what we found with [^{3}H]halichondrin B, when this maneuver led to nearly complete dissociation

of radiolabel from tubulin [33]. We concluded from this experiment that the binding of [^{3}H]DZA to the oligomeric species was tight with minimal dissociation. We also found that the [^{3}H]DZA-tubulin oligomer complex completely dissociated if passed through a size exclusion column equilibrated with 8 M urea. Thus, there is no evidence for covalent bond formation between tubulin and DZA.

4. Discussion

We have used radiolabeled DZA to study its interaction with tubulin. We initially found that it appeared to bind weakly to tubulin, with low total stoichiometry. We also found that a wide range of inhibitors of tubulin assembly had minimal or weak inhibitory effects on the binding of [^{3}H]DZA to tubulin. In attempting to enhance these inhibitory effects by preincubating the potential inhibitor with tubulin prior to addition of the [^{3}H]DZA, we observed as much as a 7-8-fold increase in the stoichiometry of binding of DZA to tubulin in the preincubated control. We explored several possible explanations for these findings. At the low [^{3}H]DZA concentrations we used, there was no precipitation of the compound in 0.1 M Mes (pH 6.9). In the absence of tubulin, we found that on average about half the [^{3}H]DZA bound to the glass reaction vessels. If tubulin was added after the [^{3}H]DZA, binding to glass was reduced to 34%. If the [^{3}H]DZA was added last, as in the preincubation experiments, binding of the radiolabeled compound to glass was reduced even further, to 22%. Since significant amounts of the [^{3}H]DZA remained in solution, we conclude that when the tubulin in the stock solutions (about 650 μM) is diluted to the final experimental concentration (usually about 4 μM) either some conformational change in the protein may occur or preexisting aggregates may disassemble. We also considered the possibility of disassembly of tubulin rings as a possible explanation, but the effects of Mg^{2+} argue against this possibility. Mg^{2+} seemed to stabilize preexisting tubulin rings and enhanced DZA-induced ring formation, but it had little effect on [^{3}H]DZA binding, and its presence in the reaction mixture did not alter enhanced DZA binding to preincubated tubulin.

When we studied binding of [^{3}H]DZA to tubulin by size exclusion filtration HPLC, we obtained a striking result. Unlike [^{3}H]halichondrin B, which bound only to 100 kDa tubulin (the αβ-heterodimer) [33], or [^{3}H]D10, which appears to bind to small tubulin oligomers prior to being found in larger complexes in the void volume [8,32], [^{3}H]DZA was recovered only in void volume complexes (> 500 kDa). This indicates either that the [^{3}H]DZA binds to pre-existing oligomers of tubulin or that the cascade reaction to larger complexes is too rapid for us to detect any intermediates. Both of these possible mechanisms also imply there can be significantly less than one DZA molecule per tubulin molecule in the complexes, as indicated by the low binding stoichiometry found in the centrifugal gel filtration assay in most experiments.

The electron microscopic evidence does not seem to clarify the mechanism of binding. We, like others [26-31], had frequently observed rings in our purified tubulin preparations. When we observed the enhanced binding of [^{3}H]DZA to preincubated tubulin, we thought that this might indicate disassembly of the rings into an active species (in terms of DZA binding), and we did observe disappearance of tubulin rings following incubation of the tubulin at room temperature. However, we found that Mg^{2+} in the reaction mixture partially prevented

the apparent disassembly of preexisting rings, but tubulin preincubated with Mg^{2+} still bound markedly increased amounts of [^{3}H]DZA, as compared with tubulin that had not been preincubated despite Mg^{2+} being in the reaction mixtures.

We also performed studies by electron microscopy of the effects of DZA on tubulin oligomerization. These studies were performed in comparison with the previously studied D10 [8]. In the present studies, reaction conditions, including addition of Mg^{2+}, had little effect on the D10-induced rings, which had an average diameter of 44-45 nm, similar to the results reported by others [11]. We should note, however, that reaction conditions can have major effects on the morphology of D10-induced aberrant polymer, including formation of tight spirals and densely packed structures that rapidly settle in the reaction vessel [8]. These are probably analogous to the precipitated polymer described in the Supplemental Materials.

This was not the case with DZA, within the limits of the studies we were able to perform with our scanty supply of the peptide. While without Mg^{2+} small numbers of single rings were formed at both pH 6.5 (diameter about 51 nm) and at pH 6.9 (dimeter about 47 nm), the number of rings formed with Mg^{2+} was substantially increased at both pH 6.5 (diameter about 56 nm) and at pH 6.9 (diameter about 55 nm). Moreover, with Mg^{2+} the thickness of the walls was noticeably increased, although the resolution in our micrographs was inadequate to be certain if there was an inner and an outer ring. Note that while Mg^{2+} in the reaction mixture dramatically increased the number of rings observed by electron microscopy and, as shown in the Supplemental Materials, the ability to recover precipitated tubulin oligomers by ultracentrifugation and to observe oligomerization by turbidimetry, the cation had no significant quantitative effect on the binding of [^{3}H]DZA to tubulin.

We also examined potential inhibition of [^{3}H]DZA binding to tubulin by a variety of inhibitors of tubulin assembly. We are focusing here in particular on vinblastine and D10 because crystal structures showed significant apparent overlap of the binding sites of both the DZA analogue DZ-2384 [16] and a number of D10 analogues [32,34,35] with the vinblastine site at the interface between two α,β-tubulin heterodimers. Originally, however, we found no inhibition of binding of [^{3}H]vinblastine or of [^{3}H]D10 to tubulin by DZA [6], and here we found no inhibition of, and even enhancement of, [^{3}H]DZA binding by vinblastine. D10, as well as cryptophycin 1, did inhibit [^{3}H]DZA binding. Without a tubulin preincubation, inhibition was negligible, but when the tubulin was preincubated, D10 became significantly more inhibitory. With 4 μM tubulin and 4 μM [^{3}H]DZA, half-maximal inhibition occurred with about 1 μM D10. Interestingly, maximum inhibition was only about 50% of [^{3}H]DZA binding. In view of the apparent superstoichiometric binding of DZA demonstrated in Fig. 3, this suggests there are at least two binding sites for DZA per tubulin in DZA-induced oligomers, only one of which is inhibited by D10 (and cryptophycin 1). If we assume this site apparently shared by D10, DZA, and vinblastine is a lower affinity site compared to that not inhibited by D10, we can perhaps rationalize the crystal data with the mutual inability of DZA and vinblastine to inhibit each other's binding to tubulin. We also reevaluated our previous observation [6] that DZA was unable to inhibit either [^{3}H]vinblastine or [^{3}H]D10 binding to tubulin, evaluating whether preincubating the tubulin before adding the ligands changed the results. As shown in Supplemental Materials, Table 3 (using analogue 2 instead of DZA, our supply of which had been exhausted), preincubating

the tubulin did not alter the results obtained: there was no inhibition by DZA analogue 2 of vinblastine or D10 binding to preincubated tubulin.

Alternatively, perhaps different binding mechanisms are involved at the low tubulin and DZA concentrations we have evaluated as opposed to the high drug concentrations and high tubulin complex concentrations required in the crystal studies. Moreover, as noted above (see Fig. 1), there are significant structural differences between DZA and DZ-2384. It is possible that there are significant differences in their binding interactions with tubulin. Finally, the different aberrant polymers induced by different compounds may mask binding sites for other compounds in unpredictable ways.

In summary, it is clear that DZA can induce formation of rings, and, under appropriate reaction conditions, can induce formation of complexes that readily form precipitates (see Supplemental Materials). What is uncertain from our studies is whether DZA binds to preexisting oligomers, presumably at substoichiometric levels, and induces a morphological change in the oligomer. Or, alternatively, whether DZA actually binds initially to αβ-tubulin heterodimers and sets off a rapid cascade leading to oligomer formation. Mechanism is further obscured by the highly variable effects of Mg^{2+} in the studies we have performed.

Supplementary Material

Refer to Web version on PubMed Central for supplementary material.

Acknowledgments

We thank Mr. Jan Endlich for assistance with the electron microscopy. This research was supported by the Developmental Therapeutics Program in the Division of Cancer Treatment and Diagnosis of the National Cancer Institute, which includes federal funds under Contract No. HHSN261200800001E. The content of this publication does not necessarily reflect the views or policies of the Department of Health and Human Services, nor does mention of trade names, commercial products, or organizations imply endorsement by the U.S. Government.

References and notes

[1]. Schwartz RE, Hirsch CF, Sesin DF, Flor JE, Chartrain M, Fromtling RE, Harris GH, Salvatore MJ, Liesch JM, Yudin K, Pharmaceuticals from cultured algae, J. Indust. Microbiol 5 (1990) 113–124.

[2]. Smith CD, Zhang X, Mooberry SL, Patterson GML, Moore RE, Cryptophycin, a new antimicrotubule agent active against drug-resistant calls, Cancer Res. 54 (1994) 3779–3784. [PubMed: 7913408]

[3]. Sasse F, Steinmetz H, Heil J, Höfle G, Reichenbach H, Tubulysins, new cytotoxic peptides from myxobacteria acting on microtubule: production, isolation, physico-chemical and biological properties. J. Antibiotics 53 (2000) 879–885. [PubMed: 11099220]

[4]. Hamel E, An overview of compounds that interact with tubulin and their effects on microtubule assembly In: Fojo AT (Ed.), Drug Discovery and Development: The Role of Microtubules in Cell Biology, Neurology, and Oncology, Humana Press, Totowa, New Jersey, 2007, pp. 1–19.

[5]. Lindquist N, Fenical W, Van Duyne GD, Clardy J, Isolation and structure determination of diazonamides A and B, unusual cytotoxic metabolites from the marine ascidian *Diazona chinensis*, J. Am. Chem. Soc 113 (1991) 2303–2304. Note that the original voucher specimen was misidentified as *D. chinensis* and was later corrected to *D. angulata*.

[6]. Cruz-Monserrate Z, Vervoort HC, Bai R, Newman DJ, Howell SB, Los G, Mullaney JT, Williams MD, Pettit GR, Fenical W, Hamel E, Diazonamide A and a synthetic structural analog: disruptive

effects on mitosis and cellular microtubules and analysis of their interactions with tubulin, Mol. Pharmacol 63 (2003) 1273–1280. [PubMed: 12761336]

[7]. Tonsing EM, Steyn PS, Osborn M, Weber K, Phomopsin-A, the causative agent of lupinosis, interacts with microtubules in vivo and in vitro, Eur. J. Cell Biol 35 (1984) 156–164.

[8]. Bai R, Taylor GF, Schmidt JM, Williams MD, Kepler JA, Pettit GR, Hamel E, Interactions of dolastatin 10 with tubulin: induction of aggregation and binding and dissociation reactions, Mol. Pharmacol 47 (1995) 965–976. [PubMed: 7746283]

[9]. Bai R, Schwartz R, Kepler JA, Pettit GR, Hamel E, Characterization of the interaction of cryptophycin 1 with tubulin: binding in the vinca domain, competitive inhibition of dolastatin 10 binding, and an unusual aggregation reaction, Cancer Res. 56 (1996) 4398–4406. [PubMed: 8813133]

[10]. Bai R, Durso NA, Sackett DL, Hamel E, Interactions of the sponge-derived antimitotic tripeptide hemiasterlin with tubulin: comparison with dolastatin 10 and cryptophycin 1, Biochemistry 38 (1999) 14301–14310.

[11]. Sackett DL, Ring polymers of tubulin induced by binding of natural antimitotic peptides, Macromol. Symp 219 (2005) 9–16.

[12]. Paull KD, Lin CM, Malspeis L, Hamel E, Identification of novel antimitotic agents acting at the tubulin level by computer-assisted evaluation of differential cytotoxicity data, Cancer Res. 52 (1992) 3892–3900. [PubMed: 1617665]

[13]. Vervoort H, Novel anticancer agents from Ascidiacea. Ph.D. dissertation, University of California at San Diego, 1999.

[14]. The IC_{50} obtained with diazonamide A in a variety of tubulin assembly reactions was among the lowest we have observed with numerous inhibitors of tubulin assembly (Hamel E, unpublished observations).

[15]. Wang G, Shang L, Burgett AWG, Harran PG, Wang X, Diazonamide toxins reveal an unexpected function for ornithine δ-amino transferase in mitotic cell division, Proc. Natl. Acad. Sci. U. S. A 104 (2007) 2068–2073. [PubMed: 17287350]

[16]. Wieczorek M, Tcherkezian J, Bernier C, Prota AE, Chaaban S, Rolland Y, Godbout C, Hancock MA, Arezzo JC, Ocal O, Rocha C, Olieric N, Hall A, Ding H, Bramoullé A, Annis MG, Zogopoulos G, Harran PG, Wilkie TW, Brekken RA, Siegel PM, Steinmetz MO, Shore GC, Brouhard GJ, Roulstan A, The synthetic diazonamide DZ-2384 has distinct effects on microtubule curvature and dynamics without neurotoxicity, Sci. Trans. Med 8 (2016) 365ra159.

[17]. Sáez-Calvo G, Sharma A, de Asís Balaguer F, Barasoain I, Rodriguez-Salarichs J, Olieric N, Muñoz-Hernández H, Berbís MA, Wendeborn S, Peñalva MA, Matesanz R, Canales A, Prota AE, Jímenez-Barbero J, Andreu JM, Lamberth C, Steinmetz MO, Díaz JF, Triazolopyrimidines are microtubule-stabilizing agents that bind the vinca inhibitor site of tubulin, Cell Chem. Biol 24 (2017) 737–750. [PubMed: 28579361]

[18]. Beyer CF, Zhang N, Hernandez R, Vitale D, Lucas J, Nguyen T, Discafani C, Ayral-Kaloustian S, Gibbons JJ, TTI-237: a novel microtubule-active compound with *in vivo* antitumor activity, Cancer Res. 68 (2008) 2292–2300. [PubMed: 18381436]

[19]. Hamel E, Lin CM, Separation of active tubulin and microtubule-associated proteins by ultracentrifugation and isolation of a component causing the formation of microtubule bundles, Biochemistry 23 (1984) 4173–4184. [PubMed: 6487596]

[20]. Grover S, Hamel E, The magnesium-GTP interaction in microtubule assembly, Eur. J. Biochem 222 (1994) 163–172. [PubMed: 8200341]

[21]. Pettit GR, Singh SB, Hogan F, Lloyd-Williams P, Herald DL, Burkett DD, Clewlow PJ, The absolute configuration and synthesis of natural (−)-dolastatin 10, J. Am. Chem. Soc 111 (1989) 5463–5465.

[22]. Pettit GR, Singh SB, Hamel E, Lin CM, Alberts DS, Garcia-Kendall D, Isolation and structure of the strong cell growth and tubulin inhibitor combretastatin A-4, Experientia 45 (1989) 209–211. [PubMed: 2920809]

[23]. Gamble WR, Durso NA, Fuller RW, Westergaard CK, Johnson TR, Sackett DL, Hamel E, Cardellina JH II, Boyd MR, Cytotoxic and tubulin-interactive hemiasterlins from *Auletta* sp. and *Siphonochalina* spp. sponges, Bioorg. Med. Chem 7 (1999) 1611–1615. [PubMed: 10482453]

[24]. Pettit GR, Cichacz ZA, Gao F, Herald CL, Boyd MR, Schmidt JM, Hooper JNA, Isolation and structure of spongistatin 1, J. Org. Chem 58 (1993) 1302–1304.

[25]. Hamel E, Lin CM, Guanosine 5'-*O*-(3-thiotriphosphate), a potent nucleotide inhibitor of microtubule assembly, J. Biol. Chem 259 (1984) 11060–11069. [PubMed: 6381495]

[26]. Voter WA, Erickson HP, Tubulin rings: curved filaments with limited flexibility and two modes of association, J. Supramol. Struct 10 (1979) 419–431. [PubMed: 513771]

[27]. Zeeberg B, Cheek J, Caplow M, Exchange of tubulin dimer into rings in microtubule assembly-disassembly, Biochemistry 19 (1980) 5078–5086. [PubMed: 7459325]

[28]. Karr TL, Purich DL, Rings are not microtubule assembly intermediates: an analysis of the lag phase in GTP-dependent self-assembly of bovine brain tubulin, Biochem. Biophys. Res. Commun 95 (1980) 1885–1889. [PubMed: 7417347]

[29]. Pantaloni D, Carlier MF, Simon C, Batelier G, Mechanism of tubulin assembly: role of rings in the nucleation process and of associated proteins in the stabilization of microtubules, Biochemistry 20 (1981) 4709–4716. [PubMed: 7295642]

[30]. Mandelkow E, Mandelkow E-M, Bordas J, Structure of tubulin rings studied by x-ray scattering using synchrotron radiation, J. Mol. Biol 167 (1983) 179–196. [PubMed: 6864800]

[31]. Shemesh A, Ginsburg A, Levi-Kalisman Y, Ringel I, Raviv U, Structure, assembly, and disassembly of tubulin single rings, Biochemistry 57 (2018) 6153–6165. [PubMed: 30247898]

[32]. We believe that the basic mechanism of the binding of dolastatin 10 to tubulin aberrant polymers is analogous to that described for vinblastine by Timasheff SN, Andreu JM, Na GC, Physical and spectroscopic methods for the evaluation of the interactions of antimitotic agents with tubulin, Pharmac. Ther 52 (1991) 191–210.The binding of the peptide to tubulin triggers a drug-induced self-association of the protein into aberrant polymers. The model of Timasheff and colleagues for vinblastine binding was confirmed in a crystal structure of a single molecule of vinblastine bound between two tubulin αβ-hetrodimers (Gigant B, Wang C, Ravelli RBG, Roussi F, Steinmetz MO, Curmi PA, Sobel A, Knossow M, Structural basis for the regulation of tubulin by vinblastine. Nature 435 (2005) 519–522). [PubMed: 15917812] Similarly, a close analogue of dolastatin 10, auristatin PE, binds in a crystal structure at the interface between the two tubulin αβ-hetrodimers, with significant but not total overlap with vinblastine (Cormier A, Marchand M, Ravelli RBG, Knossow M, Gigant B, Structural insight into the inhibition of tubulin by vinca domain peptide ligands. EMBO Rep. 9 (2008) 1101–1106). Cormier et al. reported that the vinblastine contact with the two subunits was approximately equal, 260 $Å^2$ with each subunit, while auristatin PE was in greater contact with the β-subunit (350 $Å^2$ vs 200 $Å^2$ with the α-subunit). [PubMed: 18787557] [222]

[33]. Bai R, Nguyen TL, Burnett JC, Atasoylu O, Munro MHG, Pettit GR, Smith AB III, Gussio R, Hamel E, Interactions of halichondrin B and eribulin with tubulin, J. Chem. Inf. Model 51 (2011) 1393–1404. [PubMed: 21539396]

[34]. Wang Y, Benz FW, Wu Y, Wang Q, Chen Y, Chen X, Li H, Zhang Y, Zhang R, Yang J, Structural insights into the pharmacophore of vinca domain inhibitors of microtubules, Mol. Pharmacol 89 (2016) 233–242. [PubMed: 26660762]

[35]. Waight AB, Bargsten K, Doronina S, Steinmetz MO, Sussman D, Prota AE, Structural basis of microtubule destabilization by potent auristatin antimitotics, PlosOne (2016) DOI: 10.1371/journal.pone.0160890.

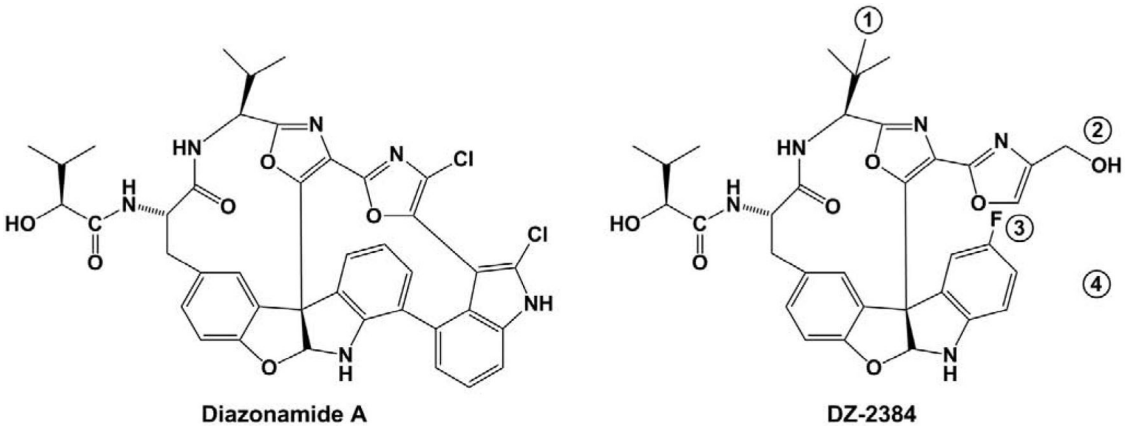

Fig. 1.

Structures of DZA and a synthetic analogue DZ-2384. DZ-2384, co-crystallized with a tubulin complex in the vinca site, differs from the natural product, as indicated, in four ways. First, a *tert*-butyl group replaces the naturally occurring isopropyl group. Second, an ethoxy group replaces the naturally occurring chloro group. Third, a fluoro group has been added. Fourth, the bridging chloroindole group has been eliminated.

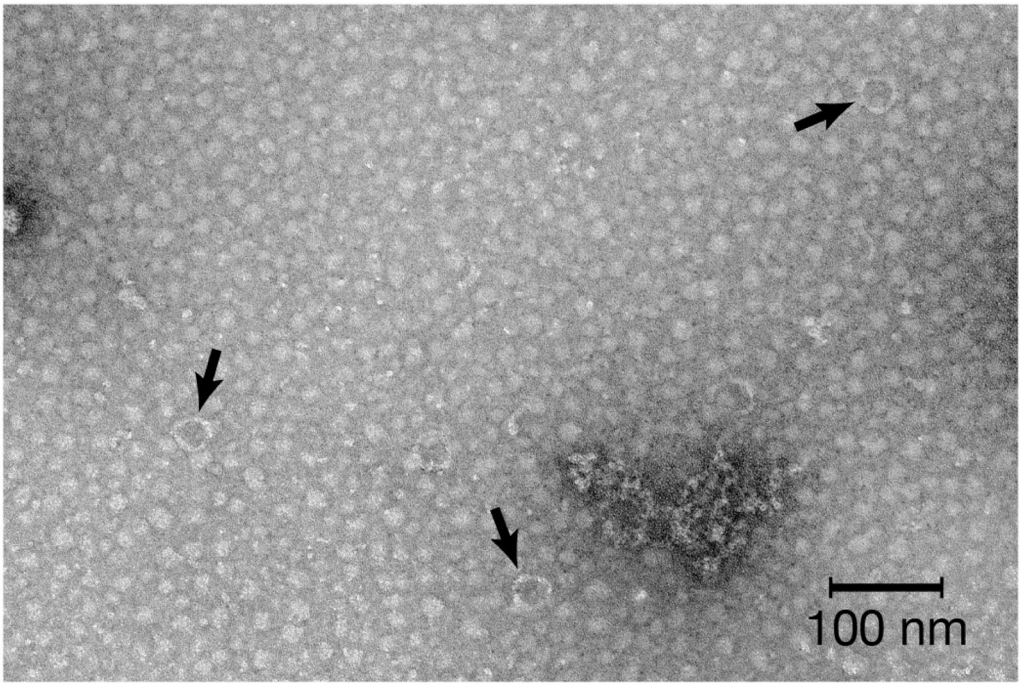

Fig. 2.

Pre-existing rings in the tubulin preparation used in studies of the binding of [^{3}H]DZA to tubulin. The reaction mixture contained 4.0 μM tubulin, 4.0% (v/v) dimethyl sulfoxide, and 0.1 M Mes (pH 6.9) at 22 °C. The grid was prepared as soon as possible after diluting the stock tubulin solution (66.5 mg/mL) into the reaction mixture. Arrows indicate some of the rings observed on the grid, and magnification as indicated.

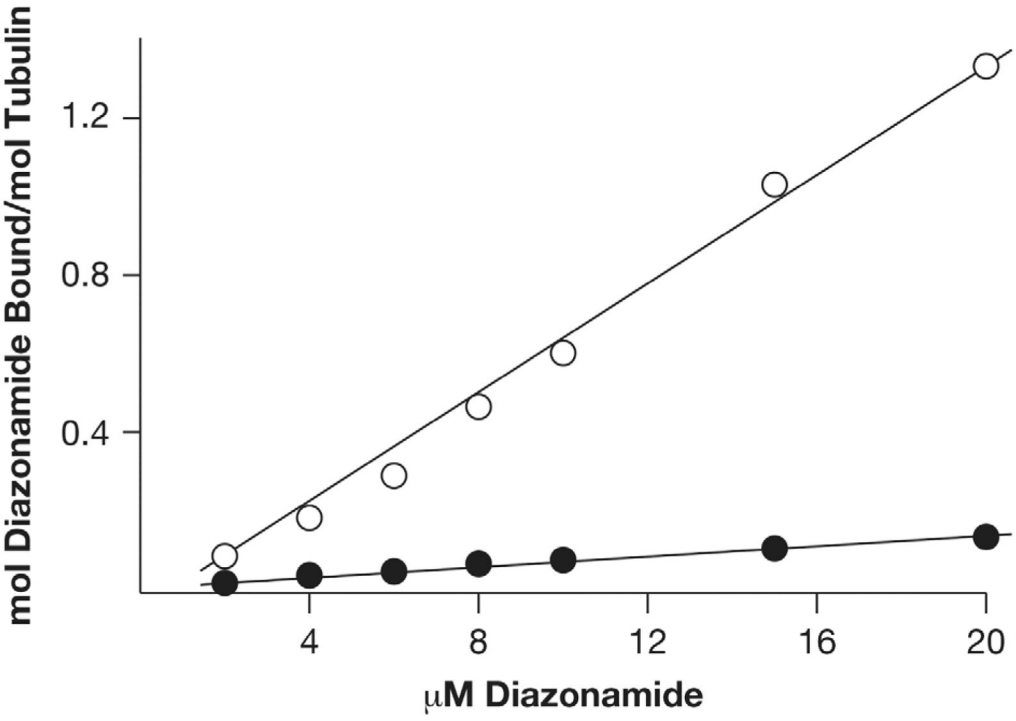

Fig. 3.

Effects of [^{3}H]DZA concentration on the binding of [^{3}H]DZA to tubulin. Each reaction mixture contained 0.1 M Mes (pH 6.9), 4.0 μM tubulin, 4.0% (v/v) dimethyl sulfoxide, and the indicated concentration of [^{3}H]DZA. The reaction mixtures were incubated for 2 h at room temperature, at which point they were applied to syringe-columns. The symbol ● represents samples in which tubulin was the last component added, and its addition initiated the incubation. The symbol ○ represents samples in which the tubulin was added prior to the [^{3}H]DZA. In these samples, the reaction mixtures were incubated for 90 min at room temperature, followed by addition of the [^{3}H]DZA with a further incubation for 2 h at room temperature prior to the samples being applied to the syringe columns.

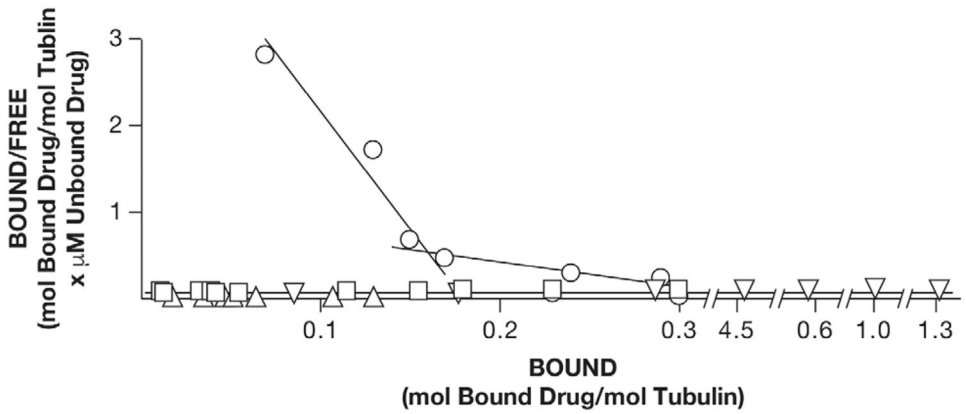

Fig. 4.

Scatchard analysis of different reaction sequences for the binding of either [^{3}H]DZA or [^{3}H]D10 to tubulin. The symbol ○ represents reaction mixtures containing 2.5 μM tubulin, 0.1 M Mes (pH 6.9), 4.0% (v/v) dimethyl sulfoxide, 0.5 mM $MgCl_2$, and varying concentrations of [^{3}H]D10 (ranging from 0.2 to 4.0 μM). D10 was the last reaction component added. Incubation was for 15 min at room temperature before the samples were applied to syringe-columns. The symbol □ represents reaction mixtures containing the same components as in the D10 reaction sequence, except that they contained varying concentrations of [^{3}H]DZA (ranging from 0.2 to 4.0 μM), which was the last reaction component added. Similar Bound/Free values were also obtained from reaction mixtures that did not contain $MgCl_2$ and/or in which the tubulin was preincubated prior to addition of the [^{3}H]DZA. The symbol Δ represents the [^{3}H]DZA containing reaction mixtures represented by the symbol ● in Fig. 3 (tubulin was the last reaction component added). The symbol ▽ represents the [^{3}H]DZA containing reaction mixtures represented by the symbol ○ in Fig. 3 (tubulin was preincubated for 90 min before [^{3}H]DZA, the last reaction component, was added).

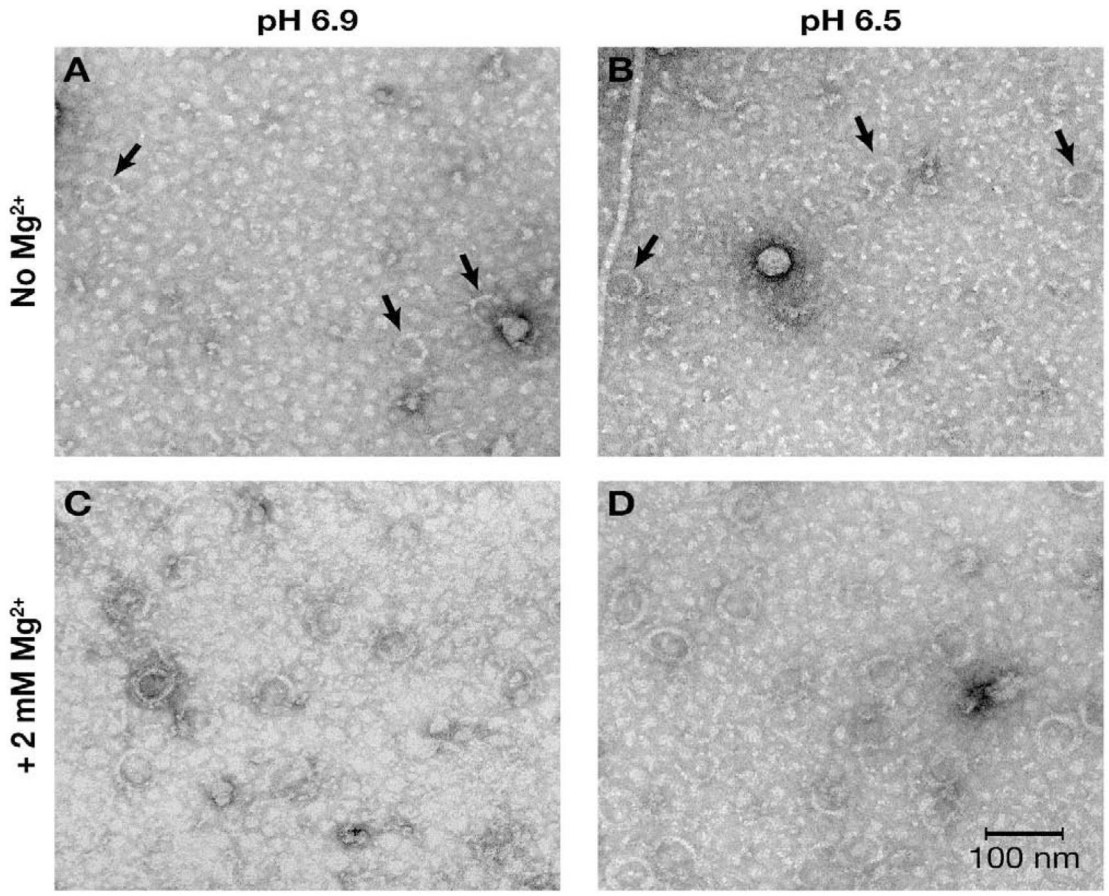

Fig. 5.

Ring formation induced by DZA. Reaction mixtures contained 0.1 M Mes at either pH 6.9 or 6.5, as indicated, and 2.0 mM $MgCl_2$, if indicated, 4.0 μM tubulin, and 4.0% (v/v) dimethyl sulfoxide and were incubated for 90 min at 22 °C in volumes of 39.7 μL. DZA (4.0 μM) was added, bringing the reaction volume to 40 μL, and, after 30 min at 22 °C, the grids were prepared. All concentrations refer to the final reaction volumes of 40 μL. Magnification as indicated in panel D. Arrows in panels A and B indicate some of the scattered rings observed in the absence of Mg^{2+}.

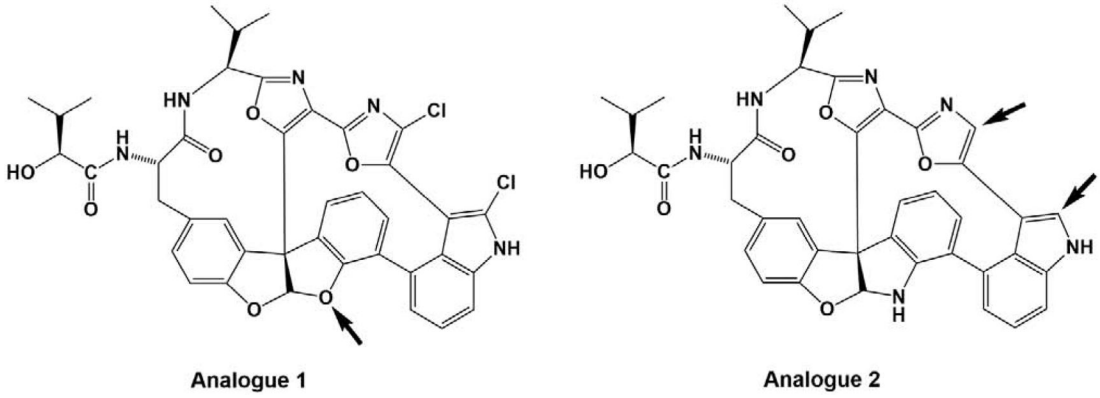

Fig. 6.

Structures of two DZA analogues that enhance, rather than inhibit, the binding of [^{3}H]DZA to tubulin. Arrows indicate structural changes from DZA.

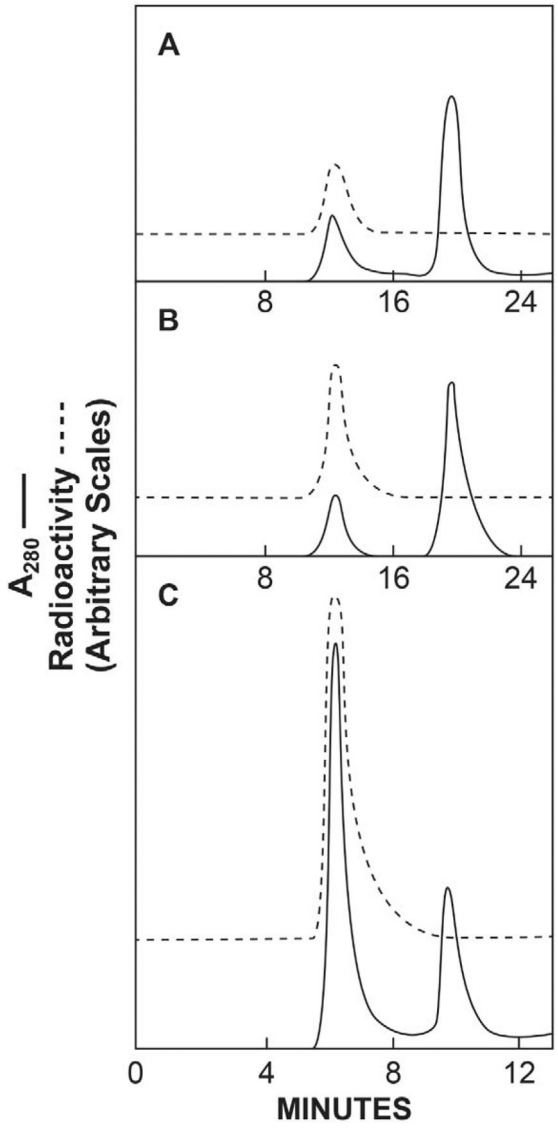

Fig. 7.

Size exclusion HPLC analysis of mixtures of tubulin and [^{3}H]DZA. In all experiments the tubulin was preincubated for 30 min at room temperature, followed by the [^{3}H]DZA for 15 min at room temperature. All reaction mixtures contained 0.1 M Mes (Ph 6.9) and 4.0% (v/v) dimethyl sulfoxide. A. The reaction mixture contained 2.0 μM tubulin and 0.5 μM [^{3}H]DZA. The flow rate was 0.5 mL/min. B. The reaction mixture contained 4.0 μM each of tubulin and [^{3}H]DZA. The flow rate was 0.5 mL/min. C. The reaction mixture contained 2.0 μM tubulin and 8.0 μM [^{3}H]DZA. The flow rate was 1.0 mL/min.

Table 1

Requirement for a Tubulin Preincubation for Maximal Binding of [^{3}H]DZA to Tubulin[a]

	mol [^{3}H]DZA bound per mol tubulin ± SE
Reaction condition 1[b]	0.083 ± 0.01
Reaction condition 2[c]	0.47 ± 0.09
Reaction condition 3[d]	0.65 ± 0.02

[a]All reaction mixtures finally contained 4.0 μM tubulin, 8.0 μM [^{3}H]DZA, 0.1 M Mes (pH 6.9), and 4.0% (v/v) dimethyl sulfoxide. Incubation after the [^{3}H]DZA was added was for 2.0 h at room temperature, at which point the samples were applied to syringe columns.

[b]For this sample, the [^{3}H]DZA was added to the reaction mixture, followed immediately by the tubulin.

[c]For this sample, the tubulin was added to the reaction mixture, followed immediately by the [^{3}H]DZA.

[d]For this sample, after addition of the tubulin to the reaction mixture, the sample was left at room temperature for 1.0 h, at which point the [^{3}H]DZA was added.

Table 2

Lack of an Effect of Mg^{2+} on the Binding of [^{3}H]DZA to Tubulin, with or without a Preincubation[a]

	---------- Mg^{2+} Concentration ----------		
	None	**0.5 mM**	**2.0 mM**
	mol [^{3}H]DZA bound per mol tubulin		
No Preincubation	0.12	0.12	0.089
1 h Preincubation	0.49	0.43	0.44

[a]All reaction mixtures finally contained 4.0 μM tubulin, 8.0 μM [^{3}H]DZA, 0.1 M Mes (pH 6.9), 4.0% (v/v) dimethyl sulfoxide, and the indicated concentration of $MgCl_2$. A 1 h preincubation at room temperature was performed prior to addition of the [^{3}H]DZA, if indicated. Incubation after the [^{3}H]DZA was added was for 2.0 h at room temperature, at which point the samples were applied to syringe columns.

Table 3

Binding of [^{3}H]DZA Is Little Affected by Incubation Time[a]

Incubation time	mol [^{3}H]DZA bound per mol tubulin ± SE
Experiment I: 4.0 μM tubulin and 8.7 μM [^{3}H]DZA	
About 20-30 s[b]	0.29 ± 0.004
2 min	0.37 ± 0.066
10 min	0.40 ± 0.01
Experiment II: 4.0 μM each tubulin and [^{3}H]DZA	
About 20-30 s[b]	0.15 ± 0.006
2 min	0.17 ± 0.005
20 min	0.20 ± 0.005
90 min	0.20 ± 0.006

[a] Reaction mixtures containing the tubulin concentration indicated, 0.1 M Mes (pH 6.9), and 4.0% (v/v) dimethyl sulfoxide were incubated for 1.5 h at room temperature. The indicated concentration of [^{3}H]DZA was added, and incubation was continued for the indicated time at room temperature. Samples placed on syringe columns swollen in 0.1 M Mes (pH 6.9).

[b] We estimate that it takes an average of 15 s to add the DZA to the reaction mixture, agitate the reaction mixture, add the sample to the syringe column, and place the syringe column in the centrifuge. The sample sinks into the dehydrated column as soon as applied, so presumably separation of bound and unbound [^{3}H]DZA occurs rapidly. In addition, it takes about 25 s to start the 6KR centrifuge and for it to reach 500 rpm.

Table 4

Effects of antitubulin agents on the binding of [^{3}H]DZA to tubulin[a] and on inhibition of pellet formation induced by DZA[b] or D10[c]

Potential inhibitor	Effect on DZA binding (% inhibition or enhancement[d] ± SE)	Effects on pellet formation (IC_{50}, μM)	
		DZA	D10
D10	55 ± 5	0.81	
DZA			27
Hemiasterlin	43 ± 3	1.1	> 60
Cryptophycin 1	59 ± 4	0.67	1.7
Halichondrin B	23 ± 6	1.4	2.6
Spongistatin 1	21 ± 7	0.90	0.15
Maytansine	9.2 ± 6	1.2	0.34
Vinblastine	E 11 ± 5	0.75	> 10
Combretastatin A-4	17 ± 3	4.6	> 60
Podophyllotoxin	20 ± 2	30	38
DZA analogue 1	E 50 ± 10		
DZA analogue 2	E 29 ± 6		

[a] Tubulin, 4.0 μM; inhibitor 30 μM; 4.0 μM [^{3}H]DZA A; 0.1 M Mes (pH 6.9), 4.0% (v/v) dimethyl sulfoxide. Inhibitor and tubulin incubated 1.5 h at room temperature (22 °C) in 148.8 μL volume; 1.2 μL of 0.5 mM [^{3}H]DZA added, and incubation continued for 40 min at room temperature. Samples were placed on syringe columns swollen in 0.1 M Mes (pH 6.9). The average control value was 0.16 ± 0.004 (S.E.) mol DZA bound per mol tubulin.

[b] Data derived from Supplemental Materials, Fig. 5, and analogous, additional experiments.

[c] Data derived from Supplemental Materials, Fig. 2, and analogous, additional experiments.

[d] Enhancement rather than inhibition indicated by “E” before the numerical value.